

[CONTRIBUTION FROM KEDZIE CHEMICAL LABORATORY, MICHIGAN STATE UNIVERSITY, EAST LANSING, MICHIGAN]

**Absorption Spectra of Sodium and Potassium in Liquid Ammonia<sup>1a</sup>**

BY ROBERT C. DOUTHIT AND JAMES L. DYE

RECEIVED FEBRUARY 12, 1960

The absorption spectra of dilute solutions of sodium and potassium in liquid ammonia were obtained as a function of concentration and temperature. The shapes of the absorption curves were found to be identical for the two metals and independent of concentration. With an increase in temperature, the absorption curve is shifted to lower energies. These results indicate that the absorption process in the near infrared ( $6800\text{ cm.}^{-1}$ ) involves the excitation of an electron in a cavity to a higher energy state and that this process is the same for dilute solutions of both metals. Sodium-ammonia solutions obeyed Beer's law within experimental error over the concentration range covered ( $3 \times 10^{-4}$  to  $4 \times 10^{-3} M$ ). Potassium solutions ( $1 \times 10^{-3}$  to  $1 \times 10^{-2} M$ ) showed a negative deviation from Beer's law. The molar absorptivity index of the sodium solutions and the extrapolated value for potassium (to zero concentration) were found to be  $4.5 \pm 0.3 \times 10^4 \text{ l. mole}^{-1} \text{ cm.}^{-1}$ . The results are explained in the light of current models for these solutions.

**Introduction**

Solutions of alkali metals in liquid ammonia are characterized by certain unusual properties which are generally similar for this group of metals but not completely identical. Although the correct structural nature of these solutions is still uncertain, many of their physical properties have been determined. The literature in this field is extensive, and the reader is referred to several articles of a review nature for a survey of the field and additional references.<sup>1b-3</sup>

Theoretical investigations concerning the nature of metal-ammonia solutions stem from the investigations of Kraus and co-workers which commenced over fifty years ago. No significant theoretical advances were made until the appearance of magnetic susceptibility data, obtained by Huster<sup>4</sup> and by Freed and Sugarman<sup>5</sup> using static fields and by Hutchison<sup>6</sup> using electron spin resonance techniques. The magnetic properties, together with conductance and density data, form the basis for the two currently popular models for the dilute solution range. These models are the 'electron cavity' model first proposed by Ogg<sup>7</sup> and the 'cluster' model proposed by Becker, Lindquist and Alder.<sup>8</sup> Both of these models explain some of the physical data adequately, but neither in its original form explains all of the facts. One of the important physical properties which can yield structural information is the absorption spectrum.

There have been many qualitative investigations of the absorption spectra of alkali metals in ammonia and amines,<sup>9-14</sup> but the only quantitative work

reported for metal-ammonia solutions involves measurements near the tail-end of the absorption band (400 to  $1000\text{ m}\mu$ ).<sup>9,15,16</sup>

Gibson and Argo<sup>9</sup> measured the concentration for two of their sodium solutions. Their data give a molar absorptivity index of  $325 \text{ l. mole}^{-1} \text{ cm.}^{-1}$  at  $500\text{ m}\mu$ . Jolly,<sup>11</sup> using the data of Gibson and Argo and measurements in the infrared, estimated the molar absorptivity index of sodium to be approximately  $4 \times 10^4 \text{ l. mole}^{-1} \text{ cm.}^{-1}$  at the infrared maximum ( $1500\text{ m}\mu$ ).

Eding<sup>15</sup> measured molar absorptivity indices for a number of sodium and potassium solutions on the visible side of the band and could find no differences in the spectra of sodium and potassium solutions. However, the values which he reports for the molar absorptivity index range from 300 to  $2700 \text{ l. mole}^{-1} \text{ cm.}^{-1}$ , so that actually only qualitative similarity was shown.

Miranda<sup>16</sup> measured the absorption spectra of sodium, potassium and calcium in ammonia from 300 to  $600\text{ m}\mu$ . He found that the molar absorptivity index for potassium was nearly 50% higher than for sodium at all wave lengths in this region in contrast to the findings reported here for the visible and near infrared regions. Miranda reports molar absorptivity indices for three solutions of each metal, with good internal agreement. However, he lists only a single concentration value: that for one of the sodium solutions, which he reports to have a molarity of 0.03285. This is more concentrated than any of the solutions reported here and the high value for the absorptivity index of potassium may reflect the presence of monomer or dimer and will be discussed later.

Shatz<sup>17</sup> has made a quantitative study of the visible absorption peak for lithium in methylaniline. Since this peak presumably is a result of the presence of dimers, the results are not directly comparable to the infrared absorption in ammonia.

The purpose of the present paper is to present some quantitative spectral data for sodium and potassium solutions in liquid ammonia in the visible and near infrared regions of the spectrum and including the absorption maximum at  $1500\text{ m}\mu$ . Particular attention has been given to the purity and stability of the solutions and to the variation

- (1) (a) Abstracted in part from a dissertation submitted by R. C. Douthit to the School for Advanced Graduate Studies of Michigan State University in partial fulfillment of the requirements for the degree of Doctor of Philosophy, 1959. This investigation received support under grant AT(11-1)-312 from the U. S. Atomic Energy Commission. (b) C. A. Kraus, *J. Chem. Educ.*, **30**, 83 (1953).
- (2) W. C. Johnson and A. W. Meyer, *Chem. Revs.*, **8**, 273 (1931).
- (3) M. C. R. Symons, *Quart. Revs. (London)*, **13**, 99 (1959).
- (4) E. Huster, *Ann. Physik*, **33**, 477 (1938).
- (5) S. Freed and N. Sugarman, *J. Chem. Phys.*, **11**, 354 (1943).
- (6) C. R. Hutchison and R. C. Pastor, *ibid.*, **21**, 1959 (1953).
- (7) R. A. Ogg, Jr., *Phys. Revs.*, **69**, 668 (1946).
- (8) E. Becker, R. H. Lindquist and B. J. Alder, *J. Chem. Phys.*, **25**, 971 (1956).
- (9) G. E. Gibson and W. L. Argo, *THIS JOURNAL*, **40**, 1327 (1918).
- (10) R. A. Ogg, Jr., *J. Chem. Phys.*, **14**, 114 (1946).
- (11) W. L. Jolly, *U.C.R.L. 2008*, U. S. Atomic Energy Commission, Washington, D. C., 1952.
- (12) H. Blades and J. W. Hodgins, *Can. J. Chem.*, **33**, 411 (1955).
- (13) G. W. A. Fowles, W. R. McGregor and M. C. R. Symons, *J. Chem. Soc.*, 3329 (1957).
- (14) G. Hohlstein and U. Wannagat, *Z. anorg. allgem. Chem.*, **288**, 193 (1957).

- (15) H. J. Eding, Ph.D. Thesis, Stanford University, 1952, D. D. No. 19, 35 (1951-1952).
- (16) F. R. Miranda, Ph.D. Thesis, Purdue University, 1957, C. A., **51**, 13426a (1957).
- (17) M. H. Shatz, Ph.D. Thesis, University of Pennsylvania, 1958, Dissertation Abstr., **18**, 2007 (1958).

of the absorption with temperature and concentration.

### Experimental

**Preparation of Solutions.**—The liquid ammonia used (Matheson Anhydrous) was dried over sodium metal in a four-liter steel cylinder. Further purification was effected by successive vacuum distillations from sodium solutions. The sodium (J. T. Baker Analyzed) and potassium (Mallinckrodt) came in hermetically sealed cans. Oxides were removed by melting *in vacuo* in the metal degassing tube shown in Fig. 1 and allowing the melt to pass through the constrictions. The tube then was broken off and introduced into the solution make-up apparatus also shown in Fig. 1. The metal again was melted *in vacuo* and allowed to run through constrictions. After seal-off of A at the bottom constriction, the entire apparatus was heated and de-gassed under vacuum for at least 6 hr. until the pressure fell to less than  $1 \times 10^{-8}$  mm. The metal was distilled into the solution make-up cell under vacuum and purified ammonia was then distilled into the large tube D (36 mm. diameter) until the light of a flashlight could just be seen through the solution. Experience showed that such a solution would have an absorbance between one and two. Further dilution could be effected by adding more ammonia to the tube. The cell was then sealed off at C. The absorption cell F was rinsed several times by immersing both tubes in a cold bath at  $-75^\circ$  and transferring the solution back and forth. Finally, about 0.5 cc. of solution was transferred into the cell F, and after sealing at E the cell was ready for the optical measurements.

**Spectrophotometric Measurements.**—A Beckman Model DK-2 Recording Spectrophotometer was used for optical measurements. Specially constructed absorption cells (American Instrument Company) of either fused silica or Pyrex with 0.1 mm. optical paths were mounted in an insulated metal vessel in order to maintain the required low temperature ( $-65$  to  $-30^\circ$ ). The details of construction are shown in Fig. 2.

The thermostated cell holder consisted of three rectangular boxes. The outer box was designed to fit the cell compartment of the spectrophotometer and was separated from the inner boxes by 'Styrofoam' insulation. The two inner boxes were joined by hollow copper tubes positioned so that the sample and reference beams could pass through the absorption cells without passing through the cooling medium. Dry air was passed through the cell compartment to prevent frost formation on the cells and windows. The coolant was absolute ethanol circulated with a Gorman-Rupp Model 210 centrifugal pump through the region between the two inner boxes and through an external bath and control system. The coolant was circulated through a Dry Ice-acetone bath and then brought to the desired temperature with electrical heaters sealed into the cooling line. Heat input was regulated with a saturable reactor circuit<sup>18</sup> using a thermistor in the fluid stream as a temperature sensing element. Temperatures near the cells could be maintained constant to  $\pm 1^\circ$  as measured with a second calibrated thermistor. It was possible to vary the temperature from room temperature to  $-65^\circ$ .

Most solutions were quite stable at low temperatures and frozen samples could be stored over Dry Ice for a week or longer with no evidence of decomposition. Repeated scanning of the spectrum showed less than 3% change in absorbance over periods of time ranging from several hours to several days, as long as the solutions were kept below  $-60^\circ$ . At higher temperatures, decomposition was more rapid but still slow enough to allow a complete trace to be made without appreciable decomposition. For example, at about  $-30^\circ$ , the decomposition rate ranged from 1 to 5% per hour. Because of this effect at the higher temperatures, data used to calculate molar absorptance indices were obtained at the lowest temperature, and the temperature dependence was examined using the ratio of absorbance to the absorbance at the maximum.

**Analysis.**—The ammonia in the large make-up tube was distilled into a small steel cylinder and weighed at room temperature. The metal residue was taken up with water and determined with the aid of a Beckman Model B Flame Photometer by comparison with standard solutions of the

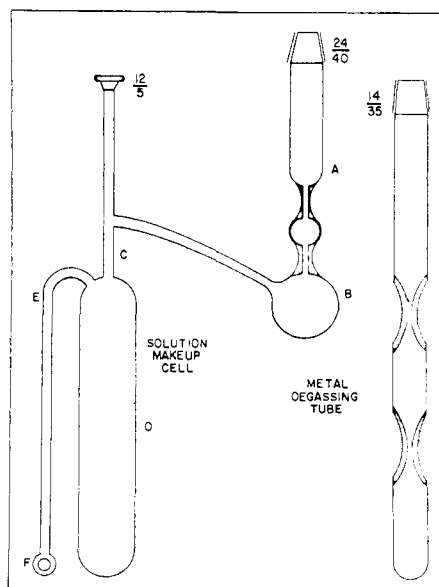


Fig. 1.

chlorides. Concentrations were expressed in moles per liter. The density of liquid ammonia at  $-65^\circ$  was obtained by extrapolation of the data of Cragoe and Harper.<sup>19</sup>

### Results

**Comparison of Line Shapes for Sodium and Potassium.**—Absorption data of sodium and potassium solutions in liquid ammonia taken from Table I are shown graphically in Fig. 3. The data are plotted as  $A/A_{\max}$  so that each curve has a maximum value of unity. In addition to allowing direct comparison of the spectral curves for different metals and concentrations, this method of plotting the results should eliminate deviations due to small amounts of decomposition. Figure 3 shows that within experimental error the line shapes are the same for sodium and potassium solutions and are nearly independent of concentration.

**Effect of Temperature on the Absorption Spectra.**—Table II gives some of the data for the temperature dependence of typical sodium and potassium spectra. The entire absorption curve is shifted to lower energies as the temperature is increased. Within experimental error, this shift is linear in temperature. The values for this displacement on the high energy side of the band (at the half-width point) are  $-9$  and  $-10 \text{ cm.}^{-1} \text{ deg.}^{-1}$  for sodium and potassium, respectively. At the maximum the values are  $-9.7$  and  $-11.5 \text{ cm.}^{-1} \text{ deg.}^{-1}$ , while on the low energy side they are  $-13$  and  $-15 \text{ cm.}^{-1} \text{ deg.}^{-1}$ , respectively. These are average values based upon eight concentrations for sodium and six concentrations for potassium. As a result of decomposition, the displacements on the sides of the bands were determined from  $A/A_{\max}$  rather than from the measured absorbances.

**Molar Absorbance Indices for Sodium and Potassium Solutions.**—Tables III and IV give the absorbance data at the wave length of the maximum and the position of the maximum for various concentrations of sodium and potassium solutions

(18) R. L. Burwell, A. H. Peterson and G. B. Rathman, *Rev. Sci. Inst.*, **19**, 608 (1948).

(19) C. S. Cragoe and D. R. Harper, *Bur. Standards Sci. Paper No. 420*, 287 (1921).

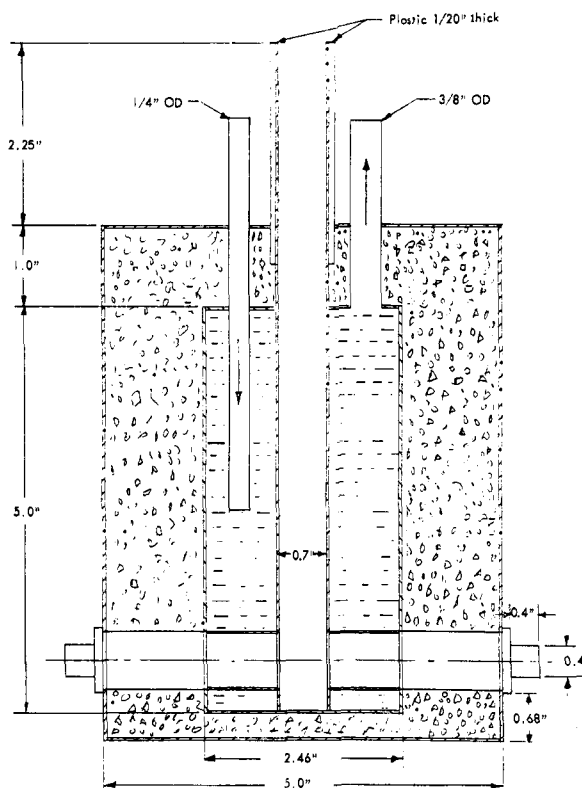
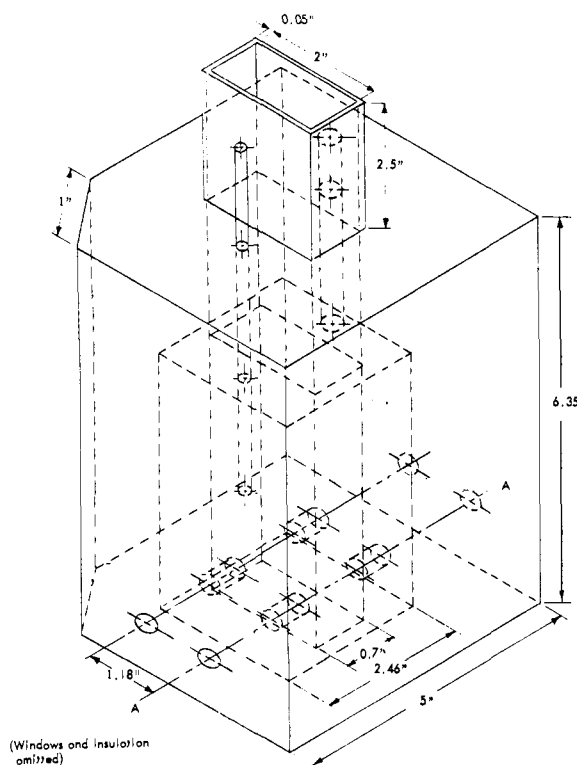


Fig. 2.—Isometric and cross-sectional views of the thermostated cell-holder.

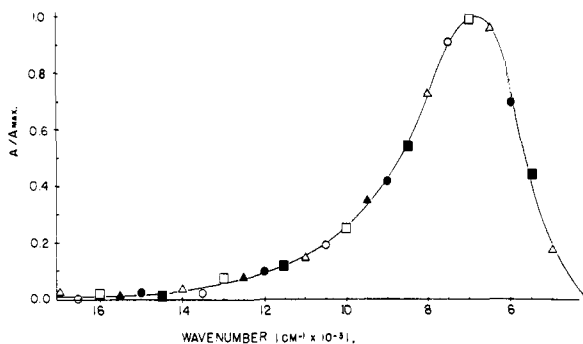


Fig. 3.—Relative absorbance,  $A/A_{\max}$ , for sodium and potassium solutions versus wave number at  $-65^\circ$ :  $\Delta$ , Na # 10;  $\circ$ , Na # 25;  $\square$ , Na # 28;  $\blacktriangle$ , K # 5;  $\bullet$ , K # 15;  $\blacksquare$ , K # 9.

at  $-65^\circ$ . Since the absorption maxima were rather broad, it was necessary to use a standardized procedure to locate the wave length of the peak. A number of horizontal lines cutting both sides of the peak were drawn at various absorbance values and the mid-points of these lines were found. These mid-points in turn formed a straight line which intersected the absorption curve at the maximum. The wave length scale was calibrated by comparison with the known absorption maxima for liquid ammonia.

The absorbance values versus concentration and the molar absorptancy indices for both metals are shown as functions of concentration in Fig. 4. The molar absorptancy indices are quite different for sodium and potassium, with the value for sodium essentially independent of concentration. The molar absorptancy index for potassium can be

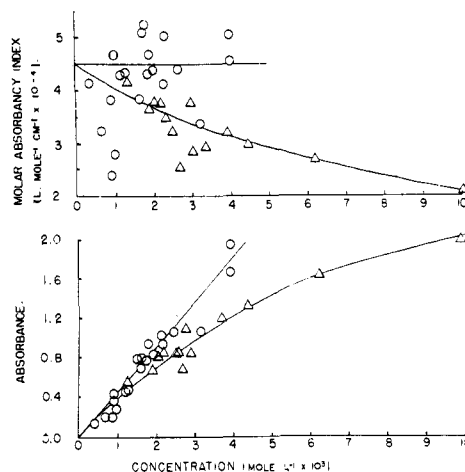


Fig. 4.—Bottom: absorbance at maximum versus concentration; top, molar absorptancy index versus concentration:  $\circ$ , sodium solutions;  $\Delta$ , potassium solutions.

reasonably extrapolated to a value at infinite dilution which is the same as that for sodium,  $4.5 \times 10^4$  l. mole $^{-1}$  cm. $^{-1}$ . Thus sodium solutions appear to obey Beer's law while potassium solutions do not. The average value of the molar absorptancy index for sodium is  $4.25 \times 10^4$  l. mole $^{-1}$  cm. $^{-1}$  with a standard deviation of  $0.77 \times 10^4$  l. mole $^{-1}$  cm. $^{-1}$ . Part of the reason for the high deviation involves the low values obtained for the molar absorptancy index at low concentrations. At low concentrations a small absolute error in absorbance or concentration yields a large error in the absorptancy index. In addition, these dilute

TABLE I

TYPICAL ABSORBANCE DATA FOR SODIUM AND POTASSIUM AT  $-65^{\circ}$ 

$\nu$ (cm. <sup>-1</sup> )	Sodium <sup>a</sup>			Potassium <sup>b</sup>		
	No. 10	No. 25	No. 28	No. 5	No. 15	No. 9
	$A/A_{max.}$	$A/A_{max.}$	$A/A_{max.}$	$A/A_{max.}$	$A/A_{max.}$	$A/A_{max.}$
16,670	0.02	0.00	0.01	0.00	0.00	0.00
14,390	.06	.00	.04	.03	.04	.01
12,500	.12	.07	.09	.08	.09	.08
11,110	.14	.14	.15	.14	.15	.14
10,000	.24	.25	.25	.27	.25	.25
9,100	.41	.42	.41	.43	.40	.41
8,330	.62	.62	.60	.64	.60	.58
7,690	.84	.85	.81	.85	.81	.80
7,140	.99	.99	.97	.99	.98	.97
6,670	.96	.99	.99	.99	.98	.98
6,250	.87	.89	.92	.89	.89	.90
5,880	.68	.70	.77	.69	.70	.69
5,550	.48	.46	.53	.48	.47	.46
5,260	.33	.27	.34	.32	.27	.34
5,000	.17	.13	.19	.19	.13	.15

<sup>a</sup> For concentrations and  $A_{max.}$  values see Table III.<sup>b</sup> For concentrations and  $A_{max.}$  values see Table IV.

TABLE II

EFFECT OF TEMPERATURE ON SODIUM AND POTASSIUM SPECTRA

$\bar{\nu}$ (cm. <sup>-1</sup> )	Na, no. 17 $C = 2.1 \times 10^{-3} M$ $t = -37^{\circ}$ to $-67^{\circ}$		K, no. 3 $C = 2.1 \times 10^{-3} M$ $t = -31^{\circ}$ to $-70^{\circ}$	
	$A_{max.} = 0.91$	$A_{max.} = 0.98$	$A_{max.} = 0.58$	$A_{max.} = 0.82$
	$A/A_{max.}$	$A/A_{max.}$	$A/A_{max.}$	$A/A_{max.}$
12,500	0.07	0.08	0.05	0.07
11,110	.13	.14	.10	.14
10,000	.21	.24	.20	.26
9,100	.34	.39	.33	.43
8,330	.53	.60	.52	.64
7,690	.75	.80	.73	.87
7,140	.94	.97	.92	.99
6,670	1.00	.99	.99	.96
6,250	0.99	.90	.99	.84
5,880	.88	.71	.93	.61
5,550	.74	.52	.80	.43
5,260	.57	.33	.61	.26
5,000	.39	.20	.45	.21
4,760	.31	.15	.36	.10
4,540	.20	.07	.24	.07

solutions are subject to greater relative decomposition than the more concentrated solutions. These difficulties are also indicated by the least-squares treatment of the *absorbance* as a function of concentration. The linear equation gives a slope of  $4.75 \times 10^4$  l. mole<sup>-1</sup> cm.<sup>-1</sup> and an intercept of  $-0.062$ . The large slope and negative intercept reflect the generally low values of absorbance at low concentrations. If runs 7, 14, 15, and 29, which give molar absorptivity indices below  $3.4 \times 10^4$  are excluded, the average value becomes  $4.53 \times 10^4$  l. mole<sup>-1</sup> cm.<sup>-1</sup> with a standard deviation of  $0.43 \times 10^4$  and a probable error of  $\pm 0.3 \times 10^4$ . From this value, we conclude that the molar absorptivity index for sodium in ammonia at the absorption maximum is  $4.5 \pm 0.3 \times 10^4$  mole<sup>-1</sup> cm.<sup>-1</sup>.

### Discussion

**Line Shape.**—Figure 3 shows that in dilute solutions the shapes of the absorption curves are the

TABLE III

MOLAR ABSORBANCY INDICES FOR SODIUM-AMMONIA SOLUTIONS AT  $-65^{\circ}$ 

Run no.	Molarity $\times 10^3$	Absorbance	Molar	$\bar{\nu}$ at peak (cm. <sup>-1</sup> )
		for $b = 10^{-2}$ cm.	absorbancy index (l./mole cm.)	
6	0.27	0.11	41,800	7095
7	0.68	.22	32,400	7060
10	1.26	.55	43,600	6900
13	1.23	.53	43,300	6940
14	0.90	.21	23,900	7180
15	1.00	.28	28,000	7000
17	2.10	.88	42,100	6835
18	0.93	.35	38,200	6970
19	1.50	.77	51,200	6890
23	1.81	.95	52,500	6765
24	1.85	.81	43,700	6885
25	1.63	.77	47,200	6880
26	1.61	.62	38,500	6830
27	1.73	.75	43,300	6795
28	3.89	1.80	46,300	6760
29	3.20	1.08	33,800	6725
30	2.09	1.06	50,600	6820
31	3.90	1.96	50,300	6790
32	0.92	0.43	47,300	6850
33	2.50	1.11	44,400	6840

TABLE IV

MOLAR ABSORBANCY INDICES FOR POTASSIUM-AMMONIA SOLUTIONS AT  $-65^{\circ}$ 

Run no.	Molarity $\times 10^3$	Absorbance	Molar	$\bar{\nu}$ at peak (cm. <sup>-1</sup> )
		for $b = 10^{-2}$ cm.	absorbancy index (l./mole cm.)	
1	2.80	1.07	38,300	6825
2	2.66	0.67	25,200	6870
3	2.14	0.81	37,800	6870
4	3.75	1.20	32,000	6700
5	2.05	0.79	38,500	6890
6	1.24	0.54	48,200	6810
7	3.27	0.94	28,700	6745
8	10 <sup>a</sup>	2.0	20,000	6715
9	6.20	1.63	26,300	6760
10	4.40	1.32	30,000	6720
11	2.48	0.81	32,600	6820
14	2.43	.86	35,400	6770
15	2.93	.83	28,300	6830
16	1.84	.68	36,900	6875

<sup>a</sup> Concentration from analysis of cell contents.

same for sodium and potassium solutions, indicating that the absorption process is the same in both solutions. The main absorption probably is not due to the monomers of Becker, Lindquist and Alder<sup>8</sup> because since the central ion would be different, these would be expected to show some differences in shape or peak position for sodium and potassium. In both the 'electron cavity' model and the 'cluster' model, the only species which is common to both sodium and potassium solutions is the solvated electron. Therefore, we are forced to conclude that the solvated electron is responsible for this absorption peak at 6800 cm.<sup>-1</sup>. The calculations of Jortner<sup>20</sup> show that the cavity model for the dilute solutions is entirely reasonable. The absorption is due to the transition ( $2p \leftarrow 1s$ ) with the energy of the  $2p$  state lower than that of a free

(20) J. Jortner, *J. Chem. Phys.*, **30**, 839 (1959).

electron. This same assignment is made by Clark, Horsfield and Symons.<sup>21</sup>

The constancy of the shape of the absorption curve with concentration indicates that the asymmetry of the high energy side of the peak is a characteristic of the absorption process for the solvated electron and is not due to an unresolved band. The possibility remains, however, that at higher concentrations shoulders might appear on the high-energy side of the peak from the presence of monomers and dimers. Symons and co-workers<sup>21</sup> have discovered two such shoulders by adding sodium iodide to dilute solutions of sodium in ammonia. These shoulders appear in the neighborhood of 12,500 and 15,000  $\text{cm}^{-1}$ . The addition of sodium ions would favor the formation of monomers and dimers and would decrease the concentration of solvated electrons. This technique avoids the masking of shoulders by the very intense infrared absorption. It is quite likely that the results of Miranda which indicated higher absorption by potassium than by sodium in the region of 16,000 to 25,000  $\text{cm}^{-1}$  are also caused by monomer and/or dimer absorption. As we shall show later, potassium tends to form dimers more readily than sodium and so would tend to have a higher absorbance in the region of the spectrum at which the dimer absorbs. Clark, Horsfield and Symons<sup>21</sup> mention that in more concentrated solutions of sodium a well-defined shoulder always is observed at about 15,000  $\text{cm}^{-1}$ . It is not clear from their statements whether this result is observed without added sodium iodide or whether the added salt is necessary. Re-examination of our spectra for both sodium and potassium (more than 400 traces at various concentrations and temperatures) showed no evidence of a shoulder on the high-energy side for concentrations as high as 0.01.

Clark, *et al.*,<sup>21</sup> do not give the values of absorbance obtained in their measurements, but these can be inferred from their graphs and the concentrations of metal and salt used. From these data one can show that even for the most concentrated sodium solution which we studied, the maximum contribution of the 12,500  $\text{cm}^{-1}$  peak to  $A/A_{\text{max}}$  would be only about 0.01. Such a contribution would be too small to detect. To check further for the presence of hidden bands, the slopes of the instrument traces of the spectra for seven sodium concentrations and six potassium concentrations were determined with the aid of a mirror, over the range 600 to 1100  $\text{m}\mu$ . The relative slopes (slope divided by  $A_{\text{max}}$ ) showed no dependence upon concentration and were the same for sodium and potassium solutions. This further substantiates the claim that the shapes of the spectra are independent of concentration and metal in this wave length region.

**Temperature Dependence.**—The spectra are quite strongly temperature-dependent with a tendency to shift to lower energies as the temperature is raised. A temperature increase tends to broaden the spectral curve and shift the peak to longer wave lengths. Since the ratios  $A/A_{\text{max}}$  and not the absolute absorbances were compared,

(21) H. C. Clark, A. Horsfield and M. C. H. Symons, *J. Chem. Soc.*, 2478 (1959). See also ref. 3.

the superposition of these two effects tends to make the apparent shift of the low-energy side of the peak larger than the shift of the high-energy side. The most significant quantity is the magnitude of the displacement of the maximum. Jortner<sup>20</sup> has given a plausible explanation for this shift based upon the temperature dependence of the dielectric constant and the cavity radius. To calculate the cavity radius, Jortner uses the temperature coefficient data of Blades and Hodgins<sup>12</sup> with which our values are in good agreement.

**Molar Absorbancy Indices.**—Figure 4 shows that the molar absorbancy indices at the maximum for sodium and potassium are different. The lower values for potassium indicate that the solvated electron is removed from the solution more readily by potassium than by sodium. The constant value of the absorbancy index for sodium indicates that the concentration of the absorbing species is constant below  $4 \times 10^{-3}$  molar. Several possible means of removal of solvated electrons in potassium solutions will be considered.

(1) The formation of  $e_2^-$  centers: It is possible that the magnetic evidence for electron pairing could be accounted for by the existence of cavities containing two electrons with opposed spins essentially free from the cation. The difference in absorbancy index for sodium and potassium rules this out as the principal cause of removal of  $e^-$  centers. The type of cation should have little effect upon the formation of  $e_2^-$  cavities. The spectra therefore afford strong evidence that this type of electron pairing is not a major contributor.

(2) The formation of ion-pairs between metal ions and cavities: One might predict the formation of ion-pairs between the metal ion and the electron in a cavity with the cavity remaining intact. This could occur to a different extent for sodium and potassium. On the basis of electrostatic considerations alone, some ion-pairing must occur, even for sodium solutions. Conductivity data for sodium<sup>22</sup> indicate that, at the highest concentrations reported here, about 20% of the ions exist as ion-pairs. The formation of an ion-pair of the type postulated should not destroy the absorption but might cause a shift of the peak with concentration. It is unlikely, therefore, that simple ion-pair formation can account for the difference in the absorbancy indices for sodium and potassium.

(3) Monomer and dimer formation: It is possible that the formation of the monomer of Becker, Lindquist and Alder<sup>8</sup> is responsible for the decrease in absorbancy index for potassium. In view of the results of Clark, Horsfield and Symons<sup>21</sup> there is undoubtedly some monomer and/or dimer formation which takes place. The higher surface charge density of the sodium ion would favor the formation of dissociated ions when compared with the potassium ion. Since we have observed no bands which can be attributed to either monomer or dimer, it is not possible to decide which of these is the most likely cause of the difference between sodium and potassium. It is possible, however, to estimate the equilibrium constant for the spin-pair-

(22) E. C. Evers and P. W. Frank, Jr., *J. Chem. Phys.*, **30**, 61 (1959).

ing reaction by assuming that *all* of the decrease in molar absorptivity index comes from dimerization, making the additional assumption that the difference between the absorptivity indices of sodium and potassium, divided by the absorptivity index of sodium gives the ratio of paired to unpaired spins. Thus the pairing constant is

$$k = \frac{\text{conc. of paired spins}}{(\text{conc. of unpaired spins})^2} = \frac{(1 - \alpha)}{2\alpha^2 C} \quad (1)$$

in which  $\alpha$  is the degree of dissociation of paired spins and is assumed to be given by

$$\alpha = \frac{\text{Absorptivity index of K}}{\text{Absorptivity index of Na}} \quad (2)$$

This gives a value of  $K = 160$  compared with the value of 500 obtained by extrapolation of the data of Hutchison<sup>6</sup> to this temperature. In view of the errors inherent in both methods, the agreement is satisfactory. The data of Hutchison for sodium are rather scanty and show more scatter than do his data for potassium, but extrapolation to  $-65^\circ$  indicates a *larger* pairing of spins for sodium than for potassium at this temperature. This is not compatible with our interpretation nor with conductance data.<sup>22</sup> It would be of interest in this connection to examine the electron spin resonance of sodium-ammonia solutions at  $-65^\circ$ .

**Shift of Peak Position with Concentration.**—The absorption maximum shifts slightly to lower energies as the concentration is increased. Figure 5 shows the measured position of the maximum plotted *versus* the value of the absorbance at the maximum. Measurements were made with reference to the ammonia absorption peaks at 1995 and 2240  $\mu$ .

Clark, *et al.*<sup>21</sup> observed a shift in the *opposite* direction with sodium iodide present, presumably because of monomer and dimer formation. The observed shift in the present case might be the result of ion-pairing. A quantitative calculation of the effect was made on the basis of this assumption.

The extent of ion-pairing was calculated by correcting the dissociation constant  $K_a$  of Evers and Frank<sup>22</sup> ( $7 \times 10^{-3}$  at  $-33.5^\circ$ ) to  $-65^\circ$  with the aid of the Bjerrum function.<sup>23</sup> In order that data for both potassium and sodium could be used, the total concentration of ion-pairs and dissociated ions was calculated from the absorbance for a path length of  $10^{-2}$  cm. and molar absorptivity index of  $4.5 \times 10^4$  as

$$[\text{Na}^+ \cdot \text{e}^-] + [\text{e}^-] = \frac{A}{4.5 \times 10^4 \times 10^{-2}} \quad (3)$$

Using the assumption that the observed peak position would be a linear function of the mole fraction of ion-pairs, the equation derived was

$$\bar{\nu} = \bar{\nu}_\infty - (\bar{\nu}_\infty - \bar{\nu}_p) \frac{K_c + 8.88 \times 10^{-3} K_c A}{4.44 \times 10^{-3} A} \quad (4)$$

in which  $\bar{\nu}_\infty$  and  $\bar{\nu}_p$  are the peak positions for dissociated electrons and electrons present in ion-pairs, respectively, and  $\bar{\nu}$  is the calculated position

(23) H. S. Harned and B. B. Owen, "The Physical Chemistry of Electrolytic Solutions," 3rd Ed., Reinhold Publishing Corporation, New York, N. Y., 1958, p. 70.

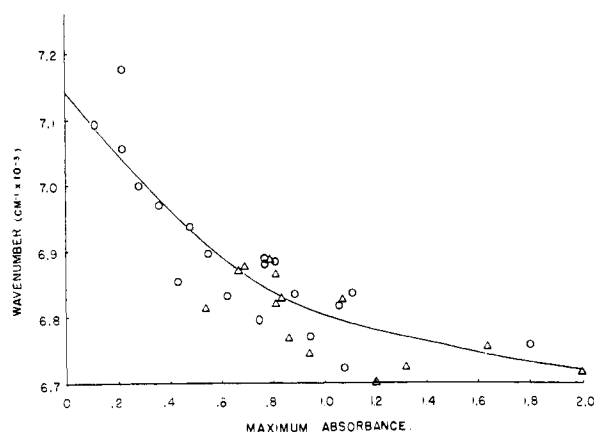


Fig. 5.—Wave number of the maximum *versus* absorbance: O, sodium solutions;  $\Delta$ , potassium solutions. Solid line calculated by equation 4.

of the peak.  $K_c = K_a/f_{\pm}^2$  is calculated from the activity constant with the aid of the Debye-Hückel equation, and  $A$  is the absorbance at the peak.

The solid line in Fig. 5 was obtained from equation 4. The end-points were fixed by adjusting  $\bar{\nu}_\infty$  and  $\bar{\nu}_p$  to 7140 and 4810  $\text{cm}^{-1}$ , respectively, but the shape of the curve is determined solely from the independent conductance data.

**Oscillator Strength.**—Integration of the composite spectral trace shown in Fig. 3 gives an oscillator strength of  $0.73 \pm 0.05$  compared with the value of  $0.65 \pm 0.05$  reported by Clark, *et al.*<sup>21</sup> The difference is due primarily to differences in the molar absorptivity indices. These authors used a value of  $4 \times 10^4$  compared with our value of  $4.5 \times 10^4$ .

**Summary of the Model.**—The model for dilute metal-ammonia solutions which is most in accord with these results and also with conductance values<sup>22</sup> is a composite of the 'cavity' and the 'cluster' models. In dilute solutions the system exists as sodium ions and electrons in spherical cavities created by polarization of the solvent. These free ions are in equilibrium with ion-pairs in which the metal ion is outside of the cavity. Perhaps the ion pair is in equilibrium with a monomer unit, in which the cation slips into the center of the cavity and the electron travels in an expanded orbital about the bound ammonia molecules. In any case, a pairing of electrons can also occur and is more favorable for potassium than for sodium. Apparently this pairing occurs through dimer formation rather than through the formation of cavities containing two electrons. The original postulate of Becker, Lindquist and Alder considered the dimer to consist of two monomer units held by exchange forces, with the electrons in expanded orbitals. The high value of the energy of absorption for the dimer ( $15,000 \text{ cm}^{-1}$ ) in solution compares favorably with the energy for the  $1^1\Sigma_u^+ \leftarrow 1^1\Sigma_g^+$  transition observed for the gas molecules<sup>24</sup> ( $14,659 \text{ cm}^{-1}$  for  $\text{Na}_2$ ,  $11,620 \text{ cm}^{-1}$

(24) G. Herzberg, "Molecular Spectra and Molecular Structure: I. Spectra of Diatomic Molecules," 2nd Ed., D. Van Nostrand Co., Inc., New York, N. Y., 1950, p. 544 and 554.

for  $K_2$ ) and suggests the possibility that the dimer in solution is essentially the same as the gas phase dimer and may not have the loosely-bound electrons postulated by the expanded-orbital model.

**Acknowledgments.**—The authors wish to thank Dr. Andrew Timnick for his advice concerning instrumentation and also wish to acknowledge the financial assistance received from the U. S. Atomic Energy Commission.

[CONTRIBUTION No. 2499 FROM THE GATES AND CRELLIN LABORATORIES OF CHEMISTRY, CALIFORNIA INSTITUTE OF TECHNOLOGY, PASADENA, CALIFORNIA]

## Protonation of Amides<sup>1</sup>

BY GIDEON FRAENKEL<sup>2</sup> AND CAFIERO FRANCONI<sup>2</sup>

RECEIVED OCTOBER 19, 1959

Evidence from cryoscopic measurements is presented that *N,N*-dimethylformamide (DMF), *N,N*-dimethylacetamide (DMA), *N*-methylacetamide (NMA) and acetamide are monoprotonated in 100% sulfuric acid. The n.m.r. spectra of a wide variety of amides in acid solution have been investigated. It is concluded that all materials examined protonate predominantly on oxygen. In aqueous acid solution proton exchange on nitrogen has been detected, the concentration of *N*-protonated species being too small to measure. A more precise method for calculating barriers to rotation for DMF is described and the values found for pure DMF and protonated DMF are  $9.6 \pm 1.5$  and  $12.7 \pm 1.5$  kcal./mole, respectively. The rate of exchange protolysis on nitrogen of DMA is first order in (DMA) and ( $H^+$ ) with a rate constant of  $400 M^{-1} \text{ sec.}^{-1}$ . The activation energy for this process for 0.4 *M* DMA in 6 *M* aqueous HCl is  $7 \pm 0.5$  kcal./mole.

### Introduction

The question as to whether amides protonate on oxygen or nitrogen has remained open for many years.<sup>3-5</sup> Of the two possibilities for a protonated amide, I and II, considerations of resonance<sup>6</sup> should favor I.



Fraenkel and Niemann<sup>7</sup> have examined qualitatively the n.m.r. spectra of several amides in acidic media. Berger, Loewenstein and Meiboom<sup>8</sup> studied the exchange protolysis of *N*-methylacetamide in acid and basic solutions using n.m.r. techniques. They both concluded that amides protonate chiefly on oxygen.

It is the purpose of this investigation to elucidate the site of protonation of amides and also to study the attendant changes in structure which occur when an amide is protonated. The technique of n.m.r. was chosen because we anticipated the n.m.r. spectra of O- and N-protonated amides, I and II, respectively, to be clearly differentiable.<sup>9</sup> For any *N,N*-dimethylcarboxamide four possibilities may be recognized: (1) *N*-protonation, II, with slow proton exchange on nitrogen should yield free rotation about the central C-N bond. The n.m.r. spectrum of the *N*-methyl groups would consist of a doublet due to spin-coupling between

the NH and  $NCH_3$  protons, respectively, and a broad line for NH. In the presence of  $D_2SO_4$  the doublet would nearly collapse since  $J_D/J_H = 1/7$ . (2) *N*-protonation with fast exchange of protons on nitrogen would produce a single line for the *N*-methyl resonance. (3) O-protonation, I, with slow exchange of protons on oxygen would produce a chemical shift between the two *N*-methyl groups, as in the case of pure *N,N*-dimethyl amides,<sup>10,11</sup> and a single line for OH. (4) O-protonation with fast exchange of protons on oxygen would yield the same spectrum for the *N*-methyl groups but no OH line. Similar considerations may be applied to other amides.

The manner in which chemical shifts and spin coupling constants in simple amides change when the amide is protonated will reflect differences in electronic configuration for the two species as well as the kinetics of exchange protolysis in acid solution.

In conjunction with these studies we have determined the degree of protonation of several amides in 100% sulfuric acid by means of cryoscopic measurements.

### Experimental

**Materials.**—All liquids were fractionally distilled before use. Their purity was determined and in certain cases improved by vapor phase chromatography through the "Aerograph" Gas Chromatographic Instrument, Wilkens Instrument Research, Inc.

The compounds *N,N*-dimethylacetamide, *N,N*-dimethylpropionamide, *N,N*-dimethylbutyramide, *N*-methylacetamide and *N*-methylformamide were obtained from Eastman Kodak Co. Mr. David Schuster kindly donated samples of *N,N*-dimethylcyclopropanecarboxamide and *N,N*-dimethylisobutyramide.

***i*-Factors.**—Cryoscopic measurements in sulfuric acid were conducted as described by O'Brien and Niemann,<sup>12</sup> our technique differing only in that liquid samples were introduced into the apparatus from a 1 cc. syringe which was weighed before and after.

**Spectrometer.**—All spectra were determined with the Varian High Resolution n.m.r. Spectrometer equipped

(1) Supported in part by U. S. Public Health Service, Grants No. RG 3823 and A 2145.

(2) Arthur A. Noyes Fellow 1958-1959.

(3) A. Hantzsch, *Ber.*, **64**, 661 (1931).

(4) A. R. Goldfarb, A. Mele and N. Gutstein, *THIS JOURNAL*, **77**, 6194 (1955).

(5) S. Mizushima, T. Simanouti, S. Nagakura, M. Tsuboi and O. Fujioka, *ibid.*, **72**, 3490 (1950).

(6) L. Pauling, "Nature of the Chemical Bond," Cornell University Press, Ithaca, New York, 1948, p. 207.

(7) G. Frankel and C. Niemann, *Proc. Natl. Acad. Sci. U. S.*, **44**, 688 (1958).

(8) A. Berger, A. Loewenstein and S. Meiboom, *THIS JOURNAL*, **81**, 62 (1959).

(9) W. D. Phillips, Research Department, Du Pont de Nemours, Delaware, has worked along similar lines (private communication).

(10) W. D. Phillips, *J. Chem. Phys.*, **23**, 1363 (1955).

(11) H. S. Gutowsky and C. H. Holm, *ibid.*, **25**, 1228 (1956).

(12) J. L. O'Brien and C. Niemann, *THIS JOURNAL*, **73**, 4264 (1951).